Published in final edited form as:

Nanotoxicology. 2013 September ; 7(6): . doi:10.3109/17435390.2012.710659.

Titanium dioxide nanoparticles activate the ATM-Chk2 DNA damage response in human dermal fibroblasts

Raju Y. Prasad[1], **Paul D. Chastain**[2], **Nana Nikolaishvili-Feinberg**[2], **Lisa M. Smeester**[1], **William K. Kaufmann**[2], and **Rebecca C. Fry**[1,2]

[1]Department of Environmental Sciences and Engineering, Gillings School of Global Public Health, University of North Carolina, Chapel Hill, NC

[2]Lineberger Comprehensive Cancer Center, School of Medicine, University of North Carolina, Chapel Hill, NC

Abstract

The use of nanoparticles in consumer products increases their prevalence in the environment and the potential risk to human health. Although recent studies have shown *in vivo* and *in vitro* toxicity of titanium dioxide nanoparticles (nano-TiO_2), a more detailed view of the underlying mechanisms of this response needs to be established. Here the effects of nano-TiO_2 on the DNA damage response and DNA replication dynamics were investigated in human dermal fibroblasts. Specifically, the relationship between nano-TiO_2 and the DNA damage response pathways regulated by ATM/Chk2 and ATR/Chk1 were examined. The results show increased phosphorylation of H2AX, ATM, and Chk2 after exposure. In addition, nano-TiO_2 inhibited the overall rate of DNA synthesis and frequency of replicon initiation events in DNA combed fibers. Taken together, these results demonstrate that exposure to nano-TiO_2 activates the ATM/Chk2 DNA damage response pathway.

Keywords

nanotoxicology; environmental toxicology; mechanistic toxicology; DNA damage response; ATM

INTRODUCTION

Titanium dioxide nanoparticles (nano-TiO_2) are used in sunscreens, paints, and cosmetics because of their high refractive index and absorptive qualities (Baan et al. 2006). The major consumer usage of nano-TiO_2 is in sunscreens which presents a highly probable dermal exposure. Studies have shown that nano-TiO_2 can cause pregnancy complications as well as DNA damage when consumed in water in mice (Yamashita et al. 2011, Trouiller et al. 2009). In addition, the genotoxicity of nano-TiO_2 has also been demonstrated *in vitro* at a variety of concentrations in several cell lines. Specifically, DNA damage and chromosome damage have been shown in human lung epithelial cells (Gurr et al. 2005), lymphoblastoid cells (Wang et al. 2007), Syrian hamster embryo fibroblasts (Rahman et al. 2002), peripheral blood lymphocytes (Kang et al. 2008) and a human fetal hepatic cell line (Shi et al. 2010). However, other studies reported negative results in these same endpoints (Hackenberg et al. 2011, Falck et al. 2009, Theogaraj et al. 2007). Despite the literature on the toxicity of nano-

Corresponding Author and Contact for Reprints: Rebecca C. Fry, Department of Environmental Sciences and Engineering, Gillings School of Global Public Health, 135 Dauer Drive, CB 7431, University of North Carolina, Chapel Hill, North Carolina, USA, Phone: (919)-843-6864, rfry@unc.edu.

Declaration of Interest: There were no competing financial interests.

TiO_2, very few studies have investigated these effects at concentrations lower than 10 μg/ml. The investigation of cellular response to DNA damage is paramount to understanding the potential carcinogenicity of a toxicant.

The data on real world nano-TiO_2 exposures in the environment are limited; however, studies have used various models and assumptions in order to estimate environmental concentrations. The U.S. Food and Drug Administration (FDA) has set a maximum concentration of titanium dioxide (by weight) at 25% without distinguishing between particle size (U.S. FDA 1999). The U.S. Environmental Protection Agency's (EPA) case study on nano-TiO_2 lists the average conventional usage of titanium dioxide in sunscreen at 2 to 15%. Furthermore, the EPA case study estimates the amount of nano-TiO_2 applied on skin as part of sunscreen for an adult outdoors for four hours is in the range of 1.0 to 4.6 g/person (or 8.0–37 mg/kg body weight) and 0.33 to 1.5 g/person (or 12–55 mg/kg body weight) for a 3-year-old infant (U.S. EPA, 2009). Additionally, it has been reported that the average consumer uses 0.5–1.5 mg of sunscreen/cm^2 skin (Srinivas et al. 2006). Assuming the average amount of nano-TiO_2 in sunscreen is ~5% w/w, the average skin exposure could be in the range of 25–75 μg nano-TiO_2/cm^2.

The cellular response to DNA damage relies on a variety of cell cycle checkpoints and DNA repair pathways (Ciccia and Elledge, 2010). S phase cells are the most vulnerable to mutations associated with DNA damage, thereby making the intra-S checkpoint important in avoiding mutagenic events associated with replicating damaged DNA. The intra-S checkpoint signaling pathways are used to slow replication and repair damaged DNA in order to minimize mutations and chromosome aberrations. Immunofluorescence microscopy of DNA combed fibers is an accepted method used to measure replication fork stalling and origin initiation (Merrick et al. 2004). This information, combined with an analysis of the major intra-S checkpoint signaling kinases ATM-Chk2 and ATR-Chk1, provides insight into the cellular response to DNA damaging agents. To date, the cellular response to nanoparticle-induced DNA damage and downstream checkpoint signaling mediated through ataxia telengiectasia-mutated (ATM) or ATM and Rad3-related (ATR) has not been investigated.

Two well-studied carcinogens, ultraviolet light (UV) and ionizing radiation (IR), have become the models for determining the intra-S checkpoint signaling response to DNA damage (Chastain et al. 2006). Ultraviolet light has been shown to increase the risk of cancer through the generation of DNA photoproducts that block DNA polymerases, the arrest of replication forks, and upregulation of ATR-Chk1 dependent DNA repair (Kaufmann 2010). Ionizing radiation causes DNA double strand breaks, with the cellular response occurring via upregulation of ATM-Chk2-dependent DNA repair (Bartek et al. 2004). If DNA damage caused by exposure to nano-TiO_2 acts primarily via the ATM-Chk2 pathway, then cells would respond to nano-TiO_2 through a pathway similar to IR. Alternatively, if exposure to nano-TiO_2 acts primarily via the ATR-Chk1 pathway, then nano-TiO_2 would act through a pathway similar to UV. IR and UV are known carcinogens, whereas, titanium dioxide is currently classified by IARC as a group 2B carcinogen or "possibly carcinogenic to humans" (IARC Monograph #93, 2010).

In this study, low, non-cytotoxic concentrations of nano-TiO_2 were tested in cultures of human dermal fibroblasts. Activation of a DNA damage response was monitored by quantification of the phosphorylation of H2AX, ATM, and Chk2 by immunocytochemistry, quantification of DNA replication dynamics using immunofluorescence microscopy of combed DNA fibers, and quantification of intra-S checkpoint signaling by western blot analysis of phosphorylation of ATM and Chk1. Using the well-established models of UV

and IR as a guide, the DNA damage response, DNA replication dynamics, and intra-S checkpoint signaling upon exposure to nano-TiO_2 were determined.

MATERIALS AND METHODS

Cell lines and Culture conditions

Human dermal fibroblasts were isolated from two independent neonatal foreskins by Dr. Jayne Boyer. Briefly, foreskins were incubated in dispase II overnight at 4 °C. The epidermis and dermis were then separated. The dermis was cut and incubated in collagenase overnight at room temperature and inactivated with media and serum. Fibroblasts were centrifuged and the cell pellet was cultured. Logarithmically growing cultures were maintained and treated from passage 3–10 in Dulbecco's modified eagle medium (Mediatech, Inc., Manassas, VA) supplemented with 10% fetal bovine serum (Invitrogen) and 1% Penicillin-Streptomycin (Thermo Scientific) at 37 °C in a humidified incubator at 5% CO_2. At 85–90% confluence, cells were trypsinized with 0.25% Trypsin-EDTA (Thermo Scientific) and reseeded at a density of 2.5×10^4 cells/cm^2. Cells were counted using a Vi-Cell XR coulter counter (Beckman Coulter).

Nanoparticle treatment conditions

Titanium dioxide nanoparticles (15 nm and 100% anatase crystal structure, as reported by the manufacturer) were purchased from Nanostructed and Amorphous Materials (NanoAmor, Houston, TX). 10–20 mg of titanium dioxide nanoparticles were weighed on the day of the experiment and suspended in the cell culture medium at a concentration of 1 mg/ml. The dispersion was sonicated using a micro-tip probe sonicator (Cole Parmer) for 2 minutes at 40% amplitude setting as recommended by the manufacturer. Sonication has been used previously in the literature to disperse nano-TiO_2 (Hackenberg et al. 2010). Cells were treated for 24 h at a final concentration of 100, 30, 10, 3, and 1 μg/ml (20 – 0.285 μg/cm^2). This preparation method was used to mimic potential dermal exposure to nano-TiO_2 from sunscreens that may contain up to 75 μg nano-TiO_2/cm^2 under current regulations. Furthermore, it has been hypothesized that the rubbing-in of sunscreen formulations with nano-TiO_2 agglomerates may act to disperse these agglomerates (McCall, 2011).

Scanning Electron Microscopy

Particle dispersions were prepared, as described earlier, at concentrations of 1 mg/ml and a drop was placed on a glass slide. The drop was allowed to dry, and the glass slide was coated with 1.5 nm of Au/Pd alloy using a Cressington 108 auto sputter coater (Cressington Scientific Instruments). The Au/Pd-coated glass slide was then adhered to the sample holder and placed inside the vacuum chamber of the SEM and observed under high vacuum.

Transmission Electron Microscopy

Transmission electron microscopy (TEM) was carried out to further visualize the intracellular internalization and localization of nano-TiO_2. Approximately 5×10^5 human dermal fibroblasts were seeded in a six well plate overnight. The following day, cells were treated with nano-TiO_2 as described above. Briefly, cell monolayers were rinsed with Dulbecco's phosphate buffered saline and fixed in 2% paraformaldehyde/2.5% glutaraldehyde/0.15M sodium phosphate at pH 7.4, for several hours or overnight. After rinsing with sodium phosphate buffer, the monolayers were fixed for 1 h in 1% osmium tetroxide/1.25% potassium ferrocyanide/0.15M sodium phosphate buffer. After rinsing in deionized water, the cells were dehydrated by going through a graded series of ethanol and embedded in Polybed 812 epoxy resin (Polysciences). The monolayers were sectioned parallel and perpendicular to the substrate at 90–100 nm using a diamond knife. Ultrathin

sections were collected on 200-mesh copper grids and viewed using a JEOL JEM 100CXII (Jeol America Inc, Peabody, MA) transmission electron microscope located at the CHANL core facility (Chapel Hill, NC). Digital images were acquired using a Gatan Orius SC1000 CCD Digital Camera and Digital Micrograph 3.11.0 (Gatan, Inc.).

Dynamic Light Scattering Measurements

Nano-TiO_2 at 1, 3, 10, 30 and 100 μg/ml in Dulbecco's modified eagle medium (Mediatech, Inc., Manassas, VA) supplemented with 10% fetal bovine serum and 1% penicillin-streptomycin were analyzed for size and zeta potential with a ZetaSizer Nano (Malvern Instruments). Settings involved a refractive index of 2.61 reflecting the titanium dioxide anatase crystal structure. To ensure the quality assurance of the measurements, each correlation function graph was analyzed to ensure a y-intercept ≤1.0. Distribution algorithm results were used in order to ensure that multiple peaks could be recorded if necessary. Each measurement was performed in triplicate, and results are the mean ± SD of three independent experiments.

Cytotoxicity

Fibroblasts treated for 24 hr with nano-TiO_2 were trypsinized as mentioned above. A cell suspension of 600 μl was placed into a ViCell XR coulter counter with specifications for measuring fibroblasts with nanoparticles. Fifty images of ~15–20 stained cells/image were stored and analyzed using ViCell 2.03 (Beckman Coulter) analysis software. Cells with blue nuclei were scored as dye-positive. Images were saved and re-analyzed to ensure there was no confounding influence of the nanoparticles on the results. The results are expressed as the mean ± SD of four independent experiments.

Immunocytochemistry analysis of pH2AX, pATM, and pChk2

Mouse monoclonal anti-phospho-ser139-H2AX (pH2AX) was purchased from Millipore (Billerica, MA), rabbit monoclonal anti-phospho-ser1981-ATM (pATM) was purchased from Epitomics (Burlingame, CA), and rabbit monoclonal anti-phospho-thr68-Chk2 (pChk2) was purchased from Cell Signaling Technology (Danvers, MA). Cells were seeded in six wells of an eight well chamber slide at a density of 2.5×10^4 cells/chamber. This allowed the examination of multiple concentrations of nano-TiO_2 on the same scaffold. After 24 hours to allow adherence to the slide, cells were treated with nano-TiO_2 for 24 hr. Cells in chamber slides were fixed in 10% formalin for ten minutes and washed with phosphate buffered saline. Immunocytochemistry was carried out in the Bond Autostainer (Leica Microsystems Inc. Norwell, MA 02061). Antigen retrieval was performed for 30 min at 100°C in Bond-Epitope Retrieval solution 1 pH-6.0 (AR9961). Slides were incubated with primary antibody for eight hours followed by antibody detection with the Bond Polymer Refine Detection System (DS9800). Stained slides were dehydrated and cover-slipped. Positive and negative controls (no primary antibody) were included for each run. The results are the mean ± SD of three independent experiments.

Stained chamber slides were digitally imaged using the Aperio ScanScope XT (Aperio Technologies, Vista, CA). Digital images were stored and analyzed within the Aperio Spectrum Database. TMALab™ (Aperio) software was used to segment each compartment of the chamber slide as an individual sector comprised of the 12 individual spots, representing randomly selected areas. The expression of each of the biomarkers was measured using Aperio Nuclear V9 (cell quantification) algorithm. Algorithm parameters, including curvature threshold and min nuclear size, have been tuned to achieve the optimal cell segmentation. The results were scored and are reported as % positive nuclei. Additionally, total nuclei scored/chamber were counted to determine differences in cell growth.

Immunofluorescence microscopy of combed DNA fibers

This protocol was performed as previously described (Chastain et al. 2006). Briefly, fibroblasts were first incubated with 10 μM iododeoxyuridine (IdU) for 10 min and after treatment with nano-TiO_2 at various concentrations for 1 hour, with 100 μM chlorodeoxyuridine (CldU) for 20 min. DNA spreads were made as described previously (Jackson and Pombo, 1998). The cells were trypsinized and resuspended in ice-cold PBS at ~200 cells/μl. To create the DNA combed fibers, 2 μl of cell suspension were mixed with 7.5 μl spreading buffer [0.5% SDS in 200 mM Tris-HCl (pH=7.4), 50 mM EDTA] on a glass slide. After 10 min, the slides were tilted at ~15° to allow the cell lysates to slowly move down the slide, resulting in DNA spreads. The slides were air-dried, fixed in 3:1 methanol/acetic acid for 2 min, and refrigerated overnight. DNA combed fibers were stained and analyzed for relative DNA synthesis and new DNA origins as previously described (Chastain et al. 2006). Relative DNA synthesis (or replicon initiation) was measured by the length of green segments in red/green tracks whereas relative origin firing was measured by the number of green only tracks (Wang et al. 2011). Results are normalized to the untreated control and expressed as mean ± SD of three independent experiments.

Western blotting

Antibodies specific for phospho-Ser 345 Chk1 (Cell Signaling Technology, Danvers, MA), Chk1 (Santa Cruz Biotechnology, Santa Cruz, CA), phospho-Ser1981 ATM (Epitomics, Burlingame, CA), ATM (Bethyl Laboratories, Montgomery, TX), phospho-Ser139 H2AX and H2AX (Millipore, Billerica, MA) were obtained. Cells were trypsinized 24 hours after treatment with nano-TiO_2 and counted using a Vi-Cell Coulter Counter (Beckman Coulter). Protein quantification was performed using the Coumassie Plus™ Protein Assay (Thermo Scientific) and NanoDrop 2000c spectrophotometer (Thermo Scientific). Preparation of whole cell extracts was done by heating cells in gel-loading buffer to 100 °C for 10 min (Bower et al. 2010). Equal amounts of protein were run on an 8–16% Precise™ protein gel (Thermo Scientific) at 120V for 1 hour at room temperature in a vertical electrophoresis system (Fisher Biotech). The polyacrylamide gel was transferred to a Hybond-P PVDF membrane (GE Healthcare) in a mini-tank electroblotter (Fisher Biotech) at 400 mA for 2 hr at 4°C. Primary antibody dilutions were all performed at 1:1000 in tris-buffered saline supplemented with 0.1% tween 20 with 5% non-fat dried milk for non-phosphorylated antibodies and tris buffered saline supplemented with 0.1% tween 20 with 5% BSA for phosphorylated antibodies. Secondary dilutions with anti-rabbit IgG HRP-linked or anti-mouse IgG HRP-linked antibodies (Cell Signaling Technology, Danvers, MA) were all performed at 1:2000 dilution in tris-buffered saline supplemented with 0.1% tween 20 with 5% non-fat dried milk. Enhanced chemiluminescence using ECL Plus reagent (GE Healthcare) and X-ray film exposure was performed as previously described (Kaufmann et al. 2003, Heffernan et al. 2002). Membranes were washed appropriately with tris-buffered saline supplemented with 0.1% tween 20 before and after primary and secondary antibody treatment. Blots were scanned and analyzed using ImageJ software (NIH). The results are the mean ± SD of three independent experiments.

Statistical Analysis

The data are presented as mean ± SD. All immunocytochemistry, replication fork stress, origin firing and western blot results were tested for significance using two-tailed t-tests comparing each concentration and positive control to the untreated control. The p value was set at 0.05 to determine significance. All data was analyzed using GraphPad Prism 5 statistical analysis software.

RESULTS

Nano-TiO_2 form agglomerates in cell culture medium

Physical characterization of nanoparticles in both dry form and dispersion has become paramount to the field of nanotoxicology (Warheit 2008, Sayes and Warheit 2009). Titanium dioxide anatase nanoparticles of 15 nm and 99.7% purity were used in this study. Analysis by scanning electron microscopy showed dry particle agglomerates (Figure 1). Additionally, transmission electron microscopy was performed on human dermal fibroblasts after 24 hr exposure (Supplemental Figure 1). Nano-TiO_2 agglomerates were internalized and primarily located in the cytoplasm of the fibroblasts, which is consistent with previously published work (Andersson et al. 2011). Dynamic light scattering was performed to determine the size of nano-TiO_2 in cell culture media (DMEM supplemented with 10% FBS and 1% Pen-Strep) (Table 1). The nanoparticle suspension showed significant agglomeration from the manufacturer's size, increasing in correlation to the mass concentration.

Concentration dependent nano-TiO_2 exposure decreases viability of human dermal fibroblasts

Assessment of cell viability was performed using the trypan dye exclusion assay. As shown in Figure 2, there was a concentration-dependent decrease in cell viability in human dermal fibroblasts treated with nano-TiO_2. Nano-TiO_2 was significantly cytotoxic at 30 and 100 μg/ml in human dermal fibroblasts after 24 h exposure (cell viability: 30 μg/ml = 58.4% ± 10.3%; 100 μg/ml = 41.2% ± 0.5%). This method was selected to enable a comparison of our results with other published studies in the literature that also found decreased cell viability at higher concentrations of nano-TiO_2 (Lewinski et al. 2008, Arora et al. 2012).

Nano-TiO_2 exposure is associated with phosphorylation of H2AX, ATM, and Chk2 as determined by immunocytochemistry

Immunocytochemical staining and analysis of phosphorylated histone 2AX (pH2AX) can be used as a marker of DNA double strand breaks (Kinner at al. 2008), but is also indicative of replication stress. As shown in Figure 3A, nano-TiO_2 produced a statistically significant increase of pH2AX as determined by % positive nuclei after 24 hr exposure at 1 and 3 μg/ml (0 μg/ml = 5.3% ± 5.13%; 1 μg/ml = 54.3% ± 12.7%; 3 μg/ml = 53% ± 8.19%). In Figure 3B, pATM showed a statistically significant increase in % positive nuclei after 24 hr exposure at 3 μg/ml (0 μg/ml = 29% ± 9.3%; 3 μg/ml = 55% ± 15.27%). In Figure 3C, pChk2 showed a statistically significant increase in % positive nuclei after 24 hr exposure at 1 and 3 μg/ml (0 μg/ml = 1% ± 0.82%; 1 μg/ml = 5% ± 0.82%; 3 μg/ml = 10.25% ± 1.26%). There were no differences in total nuclei scored/chamber between treated and untreated cells (Supplemental Table 1).

Nano-TiO_2 exposure decreases relative DNA synthesis and origin firing in human dermal fibroblasts

With two fluorescent probes used pre and post exposure to nano-TiO_2 respectively, we monitored the rates of DNA synthesis in active replicons and replicon initiation. This fiber-labeling technique has been used previously in UVC-irradiated mammalian cells (Chastain et al. 2006) as well as *Saccharomyces cerevisiae* treated with methyl methane sulfonate (MMS) and hydroxyurea (Tercero and Diffley, 2001, Shirahige et al. 1998). As shown in Figure 4A, a concentration-dependent decrease in DNA synthesis was found that reached statistical significance (relative to the untreated control) at 10, 30 and 100 μg/ml. In Figure 4B, relative origin firing (as a measure of replicon initation) also displayed a concentration-dependent decrease, displaying significance from the untreated control at 10, 30 and 100 μg/ml.

Human dermal fibroblasts respond to nano-TiO_2 exposure with activation of ATM/Chk2 DNA damage response pathway

Following the results from the immunocytochemistry analysis, we set out to examine DNA repair pathways modulated by ATM/Chk2 and ATR/Chk1 kinases in response to nano-TiO_2. To investigate these pathways, western blotting was used to determine the phosphorylation of serine residues on ATM, Chk1, and H2AX proteins (Figure 5A). Only three concentrations were tested because of the significantly reduced cell viability in the cells exposed to higher concentrations (30 and 100 μg/ml) of nano-TiO_2. Phosphorylation of H2AX was significantly higher at 1 and 10 μg/ml, but not at 3 μg/ml. Phosphorylation of ATM increased with increasing concentrations of nano-TiO_2, and was significantly higher at 3 and 10 μg/ml (Figure 5B). There was no phosphorylation of Chk1 at any concentration of nano-TiO_2 even though the positive control (UV-treatment) generated a robust p-Chk1 signal.

The phosphorylation of H2AX seen in immunocytochemistry was confirmed by western blotting with an elevated increase in pH2AX/H2AX ratio at 1, 3, and 10 μg/ml (Figure 5C). It should be noted that the positive control, UV-C, was tested at a fluence that results in ~60% cell viability (5 J/m^2) as a positive control. At such a dose, UV-C induces pATR, pH2AX, and ATR-dependent ATM phosphorylation as previously described (Stiff et al. 2006). As such, there exists cross-talk between the ATM and ATR pathways, where a sufficient UV-C dose can elicit ATR-dependent phosphorylation of ATM. However, the primary driving event for cellular response to both IR and UV-C are ATM and ATR, respectively. The increases shown in the Western blot reflect the increases seen in the immunocytochemical analysis shown in Figure 3.

DISCUSSION

This study aimed to identify whether nano-TiO_2 induces: (i) DNA double strand breaks assessed by immunocytochemistry and western blot analysis of phosphorylation of H2AX, (ii) relative DNA synthesis and origin firing using immunofluorscence microscopy of combed DNA fibers, and (iii) intra-S checkpoint signaling by immunocytochemistry and western blot analysis of phosphorylation of ATM, Chk2 and Chk1 in human dermal fibroblasts. Assessing the DNA damage response and replicon dynamics provides a critical view of the biological response to nano-TiO_2 exposure.

Potential exposure to nano-TiO_2 can occur through several routes due to their presence in sunscreens, water and aerosols. As a result, exposure can target various tissues such as the skin and the lung. For exposure through water, a model was developed to estimate predicted environmental concentrations (PEC) and predicted no-effect concentrations (PNEC) of nano-TiO_2. The reported values of 0.7 μg/L for PEC and 16 μg/L of PNEC reflected a “realistic scenario” and a “high scenario” (Mueller and Nowack, 2008). For potential lung exposure, the U.S. National Institute for Occupational Safety and Health (NIOSH) has a draft bulletin for nano-TiO_2 that recommends “0.1 mg/m^3 as time weighted average concentrations for up to 10 hr/day during a 40 hr work week” (NIOSH 2005). A study by the National Center for Computational Toxicology (NCCT) used these values to extrapolate for *in vitro* inhalation exposures and found that a range of 30–400 μg/ml was appropriate for nano-TiO_2 exposure over a lifetime (Gangwal et al. 2011). Despite these recommendations, no nanoparticle-specific recommendations have been made for consumer products.

In this study, human dermal fibroblasts were exposed to non-cytotoxic concentrations of nano-TiO_2 (e.g. 1, 3, and 10 μg/ml or 0.285, 0.857, and 2.85 $\mu g/cm^2$). The published literature on nano-TiO_2 in mouse and human fibroblasts *in vitro* describes concentrations greater than or equal to those used here (Pan et al. 2009, Jin et al. 2008, Romoser et al.

2012). Extrapolation of the EPA case study numbers gives a range of 25 – 75 μg of nano-TiO_2/cm^2 skin. Thus, the concentrations used in this study are lower than those estimated by the EPA case study for skin exposure. In intact, healthy skin, nano-TiO_2 has not been shown to penetrate past the stratum corneum (Sadrieh et al. 2010). However, studies using UVB sunburned skin showed Ti within the epidermis and superficial dermis (Monteiro-Rivere et al. 2011). Immunocompromised skin and skin with open wounds may present a potential susceptible phenotype by which human dermal fibroblasts can be exposed to nano-TiO_2.

DNA damage has been shown to occur at ≥10 μg nano-TiO_2/ml exposure in most *in vitro* studies (Singh et al. 2009). However, most nanogenotoxicity studies use the alkaline single cell gel (comet) and micronucleus assays to assess DNA damage and chromosome breakage, respectively. It has been shown previously that phosphorylation of H2AX is not only a marker for double strand breaks, but it is also critical for recruitment of repair factors after DNA damage (Paull et al. 2000). A recent study by Trouiller et al. found pH2AX to be the most sensitive marker of DNA damage in response to nano-TiO_2 exposure (Trouiller et al. 2009). This former study was performed *in vivo* with concentrations of nano-TiO_2 ranging from 60–600 μg/ml in drinking water causing statistically significant increases in pH2AX in bone marrow. The results from our study demonstrate increases in pH2AX after 24 h exposure in human dermal fibroblasts *in vitro* using immunocytochemistry and western immunoblotting.

Upon exposure to agents that damage DNA, cells can initiate a host of responses that include the reduction of the rate of synthesis in order to minimize the risk of developing mutations. Here we found reduced rates of DNA synthesis in active replicons and reduced origin firing after one hour incubation with concentrations at and above 10 μg/ml. To our knowledge, this is the first study to look at replication dynamics in DNA combed fibers after exposure to nano-TiO_2. Such a reduced rate of synthesis after exposure may be the result of cell cycle checkpoint activation in response to DNA damage. Similar to our results for nano-TiO_2, IR has been shown to inhibit DNA synthesis through ATM-Chk2 signaling (Painter and Young, 1980, Falck et al. 2001). Other studies have shown a change in cell cycle progression as a result of nanoparticle exposure (Huang et al. 2009, Wu et al. 2010). More studies are necessary to investigate the effects of nanoparticles on DNA replication and cell cycle dynamics.

Cellular pathways that are altered in response to nanoparticle exposure have not been studied thoroughly. It has been shown that the phosphorylation of p53 and p53-transactivation targets such as p21 and Bax occur as a result of a high concentration (50 μg/ml) of nano-TiO_2 exposure in human peripheral blood lymphocytes (Kang et al. 2008). Here, we sought to determine whether the cellular response to DNA damage from lower concentrations of nano-TiO_2 was through a mechanism similar to IR and/or UV exposure. IR-induced S-checkpoint signaling is dependent upon ATM recognizing DNA double strand breaks and initiating a cascade that inhibits replicon initiation and DNA synthesis in active replicons (Falck et al. 2001). ATM phosphorylates Chk2 and pChk2 proceeds to phosphorylate Cdc25A to induce ubiquitin-mediated proteolysis if Cdc25A, resulting in inhibition of DNA synthesis (Busino et al. 2003). UV-induced S-checkpoint signaling is shown to be dependent upon ATR activation at replication forks that are stalled at UV-induced DNA 6-4 photoproducts (Kaufmann 2010). Once activated, ATR acts through Chk1 to inhibit replicon initiation and induce S phase arrest (Heffernan et al. 2007). While these paradigms largely hold true, in instances of high dose exposures to UV-C and IR, an ATR-dependent phosphorylation of ATM and ATM-dependent phosphorylation of ATR can occur (Stiff et al. 2006). In our study, the absence of a detectable signal of p-Chk1 in TiO_2 nanoparticle-treated cells suggests that ATR was not activated.

From previous studies, nano-TiO_2 has been shown to induce DNA lesions through reactive oxygen species (ROS) as assessed by the formamido-pyrimidine-DNA-glycosylase (Fpg) comet assay *in vitro*, which recognizes oxidatively damaged purines (Shukla et al. 2011a, Shukla et al. 2011b). In addition, it has been shown that exposure to nano-TiO_2 induces DNA radicals using an immuno spin trapping technique (Kitchin et al. 2011). ROS and radical induced DNA damage, if clustered, can yield DNA double strand breaks that can activate the ATM-Chk2 signaling pathway. However, studies have also shown that some types of nano-TiO2 are weak producers of ROS (Moller et al. 2010). More studies should be performed to specifically examine the types and amounts of ROS produced by exposure to nano-TiO2.

The data shown here demonstrate that nano-TiO_2 induces phosphorylation of H2AX, a marker of DNA damage. Relating the findings of our study with known mechanisms established for standard responses to UV and IR, it can be seen that after 24 hr exposure, nano-TiO_2 acts primarily through the phosphorylation of ATM/Chk2, in a manner similar to IR. In addition, we show that the ATR/Chk1 pathway is not activated in response to nano-TiO_2 exposure. These results demonstrate that exposure to nano-TiO_2 induces activation of the ATM/Chk2 DNA damage signaling pathway (Figure 6).

CONCLUSIONS

This study examined the effects of nano-TiO_2 on DNA damage response pathways including phosphorylation of H2AX, replicon dynamics, and intra-S checkpoint signaling. The results indicate that human dermal fibroblasts exposed to nano-TiO_2 respond primarily via the ATM/Chk2 pathway. Future research on the effects of nano-TiO_2 on replication dynamics and DNA damage response are necessary if the impact on human health is to be fully understood.

Supplementary Material

Refer to Web version on PubMed Central for supplementary material.

Acknowledgments

The authors would like to thank Dr. Jayne Boyer, Wallace Ambrose at the Chapel Hill Analytical and Nanofabrication Laboratory, and Stephanie Smith-Roe of the Kaufmann laboratory. In addition, we thank Mark Olorvida and Bentley Midkiff of the Translational Pathology Core Facility at Lineberger Comprehensive Cancer Center at the University of North Carolina at Chapel Hill for assistance with the study. This Body on a Chip project was supported by a Gillings Innovation Laboratory award from the UNC Gillings School of Global Public Health. In addition, this research was supported in part by a grant from the National Institute of Environmental Health Sciences (P30ES010126, P42ES005948, and ES019315).

Abbreviations

Nano-TiO_2	Titanium Dioxide nanoparticles
DLS	Dynamic Light Scattering
TEM	Transmission electron microscopy
SEM	Scanning electron microscopy
ATM	ataxia telengiectasia-mutated
ATR	ATM and Rad3-related
H2AX	H2A histone family, member X

IR	ionizing radiation
UV	ultraviolet light

References

Andersson PO, Lejon C, Ekstrand-Hammarstrom B, Akfur C, Ahlinder L, Bucht A, et al. Polymorph- and size-dependent uptake and toxicity of TiO nanoparticles in living lung epithelial cells. Small. 2011; 7(4):514–523. [PubMed: 21265017]

Arora S, Rajwade JM, Paknikar KM. Nanotoxicology and in vitro studies: the need of the hour. Toxicol Appl Pharmacol. 2012; 258(2):151–65. [PubMed: 22178382]

Bartek J, Lukas C, Lukas J. Checking on DNA damage in S phase. Nat Rev Mol Cell Biol. 2004; 5(10):792–804. [PubMed: 15459660]

Bower JJ, Zhou Y, Zhou T, Simpson DA, Arlander SJ, Paules RS, et al. Revised genetic requirements for the decatenation G2 checkpoint: The role of ATM. Cell Cycle. 2010; 9(8):1617–1628. [PubMed: 20372057]

Busino L, Donzelli M, Chiesa M, Guardavaccaro D, Ganoth D, Dorrello NV, et al. Degradation of Cdc25A by beta-TrCP during S phase and in response to DNA damage. Nature. 2003; 426(6962): 87–91. [PubMed: 14603323]

Chastain PD 2nd, Heffernan TP, Nevis KR, Lin L, Kaufmann WK, Kaufman DG, et al. Checkpoint regulation of replication dynamics in UV-irradiated human cells. Cell Cycle. 2006; 5(18):2160–2167. [PubMed: 16969085]

Ciccia A, Elledge SJ. The DNA damage response: making it safe to play with knives. Mol Cell. 2010; 40:179–204. [PubMed: 20965415]

Falck GC, Lindberg HK, Suhonen S, Vippola M, Vanhala E, Catalan J, et al. Genotoxic effects of nanosized and fine TiO2. Hum Exp Toxicol. 2009; 28(6–7):339–352. [PubMed: 19755445]

Falck J, Mailand N, Syljuasen RG, Bartek J, Lukas J. The ATM-Chk2-Cdc25A checkpoint pathway guards against radioresistant DNA synthesis. Nature. 2001; 410(6830):842–7. [PubMed: 11298456]

FDA (U.S. Food and Drug Administration). Final Rule for Sunscreen Drug Products for Over-the-Counter Human Use. 1999. 64 FR 27666; codified in 21 CFR 352. Retrieved June 2 2009, from http://www.access.gpo.gov/nara/cfr/waisidx_08/21cfr352_08.html

Gangwal S, Brown JS, Wang A, Houck KA, Dix DJ, Kavlock RJ, Cohen Hubal EA. Informing Selection of Nanomaterial Concentrations for ToxCast *In Vitro* Testing based on Occupational Exposure Potential. Environ Health Perspect. 2011; 119(11):1539–46. [PubMed: 21788197]

Gurr JR, Wang AS, Chen CH, Jan KY. Ultrafine titanium dioxide particles in the absence of photoactivation can induce oxidative damage to human bronchial epithelial cells. Toxicology. 2005; 213(1–2):66–73. [PubMed: 15970370]

Hackenberg S, Friehs G, Froelich K, Ginzkey C, Koehler C, Scherzed A, et al. Intracellular distribution, geno- and cytotoxic effects of nanosized titanium dioxide particles in the anatase crystal phase on human nasal mucosa cells. Toxicol Lett. 2010; 195(1):9–14. [PubMed: 20206675]

Hackenberg S, Friehs G, Kessler M, Froelich K, Ginzkey C, Koehler C, et al. Nanosized titanium dioxide particles do not induce DNA damage in human peripheral blood lymphocytes. Environ Mol Mutagen. 2011; 52(4):264–268. [PubMed: 20740634]

Heffernan TP, Simpson DA, Frank AR, Heinloth AN, Paules RS, Cordeiro-Stone M, et al. An ATR- and Chk1-dependent S checkpoint inhibits replicon initiation following UVC-induced DNA damage. Mol Cell Biol. 2002; 22(24):8552–8561. [PubMed: 12446774]

Heffernan TP, Unsal-Kacmaz K, Heinloth AN, Simpson DA, Paules RS, Sancar A, et al. Cdc7-Dbf4 and the human S checkpoint response to UVC. J Biol Chem. 2007; 282(13):9458–9468. [PubMed: 17276990]

Huang S, Chueh PJ, Lin YW, Shih TS, Chuang SM. Disturbed mitotic progression and genome segregation are involved in cell transformation mediated by nano-TiO2 long-term exposure. Toxicol Appl Pharmacol. 2009; 241(2):182–194. [PubMed: 19695278]

IARC Monograph 93 (Titanium Dioxide). http://monographs.iarc.fr/ENG/Monographs/PDFs/93-titaniumdioxide.pdf

Jackson DA, Pombo A. Replicon clusters are stable units of chromosome structure: evidence that nuclear organization contributes to the efficient activation and propagation of S phase in human cells. J Cell Biol. 1998; 140(6):1285–1295. [PubMed: 9508763]

Jin CY, Zhu BS, Wang XF, Lu QH. Cytotoxicity of titanium dioxide nanoparticles in mouse fibroblast cells. Chem Res Toxicol. 2008; 21(9):1871–7. [PubMed: 18680314]

Kang SJ, Kim BM, Lee YJ, Chung HW. Titanium dioxide nanoparticles trigger p53-mediated damage response in peripheral blood lymphocytes. Environ Mol Mutagen. 2008; 49(5):399–405. [PubMed: 18418868]

Kaufmann WK. The human intra-S checkpoint response to UVC-induced DNA damage. Carcinogenesis. 2010; 31(5):751–65. [PubMed: 19793801]

Kaufmann WK, Heffernan TP, Beaulieu LM, Doherty S, Frank AR, Zhou Y, et al. Caffeine and human DNA metabolism: the magic and the mystery. Mutat Res. 2003; 532(1–2):85–102. [PubMed: 14643431]

Kinner A, Wu W, Staudt C, Iliakis G. Gamma-H2AX in recognition and signaling of DNA double-strand breaks in the context of chromatin. Nucleic Acids Res. 2008; 36(17):5678–5694. [PubMed: 18772227]

Kitchin KT, Prasad RY, Wallace K. Oxidative stress studies of six TiO2 and two CeO2 nanomaterials: immuno-spin trapping results with DNA. Nanotoxicology. 2011; 5(4):546–56. [PubMed: 21142840]

Lewinski N, Colvin V, Drezek R. Cytotoxicity of nanoparticles. Small. 2008; 4(1):26–49. [PubMed: 18165959]

McCall MJ. Environmental, health and safety issues: Nanoparticles in the real world. Nat Nanotechnol. 2011; 6(10):613–4. [PubMed: 21979234]

Merrick CJ, Jackson D, Diffley JF. Visualization of altered replication dynamics after DNA damage in human cells. J Biol Chem. 2004; 279(19):20067–20075. [PubMed: 14982920]

Moller P, Jacobsen NR, Folkmann JK, Danielsen PH, Mikkelsen L, Hemmingsen JG, Vesterdal LK, Forchhammer L, Wallin H, Loft S. Role of oxidative damage in toxicity of particulates. Free Radic Res. 2010; 44(1):1–46. [PubMed: 19886744]

Monteiro-Rivere NA, Wiench K, Landsiedel R, Schulte R, Inman AO, Riviere JE. Safety evaluation of sunscreen formulation containing titanium dioxide and zinc oxide nanoparticles in UVB sunburned skin: an *in vitro* and *in vivo* study. Tox Sci. 2011; 123(1):264–280.

Mueller NC, Nowack B. Exposure modeling of engineered nanoparticles in the environment. Environ Sci Technol. 2008; 42:4447–4453. [PubMed: 18605569]

NIOSH (National Institute for Occupational Safety and Health). Approaches to Safe Nanotechnology: Managing the Health and Safety Concerns Associated with Engineered Nanomaterials. 2009. Retrieved June 2,2009, from http://cdc.gov/niosh/docs/2009-125/

Pan Z, Lee W, Slutsky L, Clark RA, Pernodet N, Rafailovich MH. Adverse effects of titanium dioxide nanoparticles on human dermal fibroblasts and how to protect cells. Small. 2009; 5(4):511–20. [PubMed: 19197964]

Painter RB, Young BR. Radiosensitivity in ataxia-telangiectasia: a new explanation. Proc Natl Acad Sci USA. 1980; 77(12):7315–7. [PubMed: 6938978]

Paull TT, Rogakou EP, Yamazaki V, Kirchgessner CU, Gellert M, Bonner WM. A critical role for histone H2AX in recruitment of repair factors to nuclear foci after DNA damage. Curr Biol. 2000; 10(15):886–95. [PubMed: 10959836]

Rahman Q, Lohani M, Dopp E, Pemsel H, Jonas L, Weiss DG, et al. Evidence that ultrafine titanium dioxide induces micronuclei and apoptosis in Syrian hamster embryo fibroblasts. Environ Health Perspect. 2002; 110(8):797–800. [PubMed: 12153761]

Romoser AA, Figueroa DE, Sooresh A, Scriber K, Chen PL, Porter W, Criscitiello MF, Sayes CM. Distinct immunomodulatory effects of a panel of nanomaterials in human dermal fibroblasts. Tox Lett. 2012; 210:293–301.

Sadrieh N, Wokovich AM, Gopee NV, Zheng J, Haines D, Parmiter D, Siitonen PH, Cozart CR, Patri AK, McNeil SE, Howard PC, Doub WH, Buhse LF. Lack of significant dermal penetration of

titanium dioxide from sunscreen formulations containing nano- and submicron-size TiO_2 particles. Tox Sci. 2010; 115(1):156–166.

Sayes CM, Warheit DB. Characterization of nanomaterials for toxicity assessment. Wiley Interdiscip Rev Nanomed Nanobiotechnol. 2009; 1(6):660–670. [PubMed: 20049823]

Shi Y, Zhang JH, Jiang M, Zhu LH, Tan HQ, Lu B. Synergistic genotoxicity caused by low concentration of titanium dioxide nanoparticles and p,p′-DDT in human hepatocytes. Environ Mol Mutagen. 2010; 51(3):192–204. [PubMed: 19708068]

Shirahige K, Hori Y, Shiraishi K, Yamashita M, Takahashi K, Obuse C, et al. Regulation of DNA-replication origins during cell-cycle progression. Nature. 1998; 395(6702):618–621. [PubMed: 9783590]

Shukla RK, Sharma V, Pandey AK, Singh S, Sultana S, Dhawan A. ROS-mediated genotoxicity induced by titanium dioxide nanoparticles in human epidermal cells. Toxicol In Vitro. 2011; 25(1):231–41. [PubMed: 21092754]

Shukla RK, Kumar A, Gurbani D, Pandey AK, Singh S, Dhawan A. TiO(2) nanoparticles induce oxidative DNA damage and apoptosis in human liver cells. Nanotoxicology. 2011 Nov 2. Epub ahead of print.

Singh N, Manshian B, Jenkins GJ, Griffiths SM, Williams PM, Maffeis TG, et al. NanoGenotoxicology: the DNA damaging potential of engineered nanomaterials. Biomaterials. 2009; 30(23–24):3891–3914. [PubMed: 19427031]

Srinivas CR, Lal S, Thirumoorthy M, Sundaram SV, Karthick PS. Sunscreen application: Not less, not more. Indian J Dermatol Venerol Leprol. 2006; 72:306–7.

Stiff T, Walker SA, Cerosaletti K, Goodarzi AA, Petermann E, Concannon P, O'Driscoll M, Jeggo PA. ATR-dependent phosphorylation and activation of ATM in response to UV treatment or replication fork stalling. EMBO J. 2006; 25(24):5775–82. [PubMed: 17124492]

Tercero JA, Diffley JF. Regulation of DNA replication fork progression through damaged DNA by the Mec1/Rad53 checkpoint. Nature. 2001; 412(6846):553–557. [PubMed: 11484057]

Theogaraj E, Riley S, Hughes L, Maier M, Kirkland D. An investigation of the photo-clastogenic potential of ultrafine titanium dioxide particles. Mutat Res. 2007; 634(1–2):205–219. [PubMed: 17855159]

Trouiller B, Reliene R, Westbrook A, Solaimani P, Schiestl RH. Titanium dioxide nanoparticles induce DNA damage and genetic instability in vivo in mice. Cancer Res. 2009; 69(22):8784–8789. [PubMed: 19887611]

U.S. EPA. Nanomaterial Case Studies: Nanoscale Titanium Dioxide in Water Treatment and in Topical Sunscreen (Final). U.S. Environmental Protection Agency; Washington, DC: 2010. EPA/600/R-09/057F

Vilenchik MM, Knudson AG. Endogenous DNA double-strand breaks: production, fidelity of repair, and induction of cancer. Proc Natl Acad Sci USA. 2003; 100:12871–12876. [PubMed: 14566050]

Wang JJ, Sanderson BJ, Wang H. Cyto- and genotoxicity of ultrafine TiO2 particles in cultured human lymphoblastoid cells. Mutat Res. 2007; 628(2):99–106. [PubMed: 17223607]

Warheit DB. How meaningful are the results of nanotoxicity studies in the absence of adequate material characterization? Toxicol Sci. 2008; 101(2):183–185. [PubMed: 18300382]

Wu J, Sun J, Xue Y. Involvement of JNK and P53 activation in G2/M cell cycle arrest and apoptosis induced by titanium dioxide nanoparticles in neuron cells. Toxicol Lett. 2010; 199(3):269–276. [PubMed: 20863874]

Wang Y, Chastain P, Yap PT, Cheng JZ, Kaufman D, Guo L, Shen D. Automated DNA fiber tracking and measurement. Proc IEEE ISBI. 2011:1349–1352.

Xia T, Kovochich M, Brant J, Hotze M, Sempf J, Oberley T, et al. Comparison of the abilities of ambient and manufactured nanoparticles to induce cellular toxicity according to an oxidative stress paradigm. Nano Lett. 2006; 6(8):1794–1807. [PubMed: 16895376]

Yamashita K, Yoshioka Y, Higashisaka K, Mimura K, Morishita Y, Nozaki M, et al. Silica and titanium dioxide nanoparticles cause pregnancy complications in mice. Nat Nanotechnol. 2011; 6(5):321–328. [PubMed: 21460826]

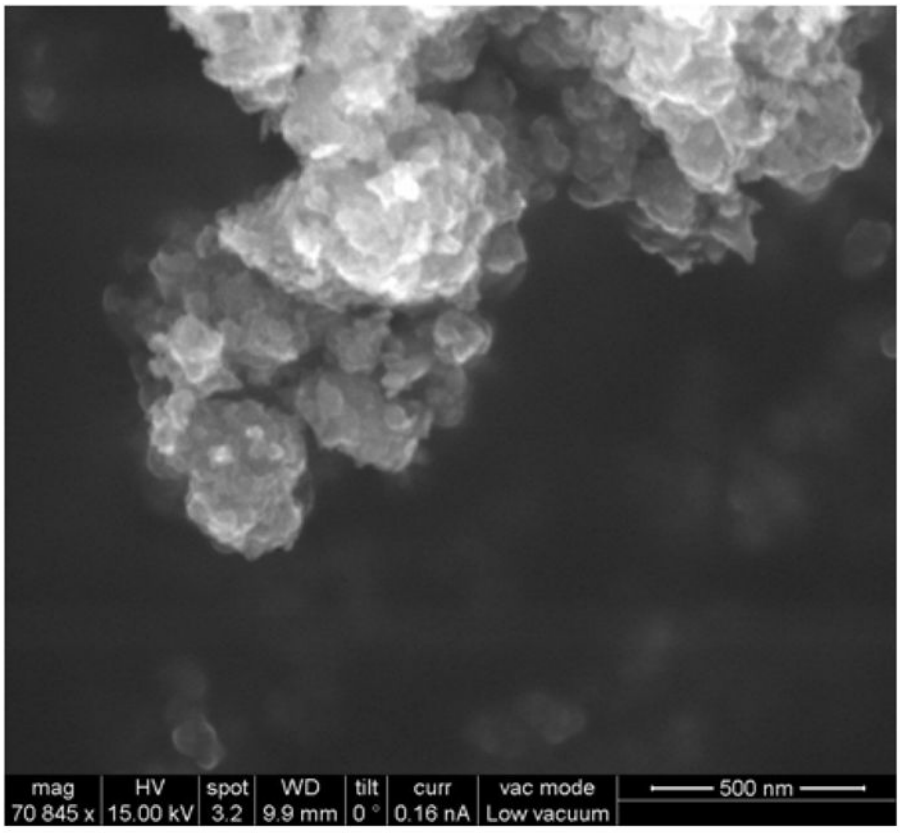

Figure 1.
Physical characterization of titanium dioxide nanoparticles in dry form using scanning electron microscopy.

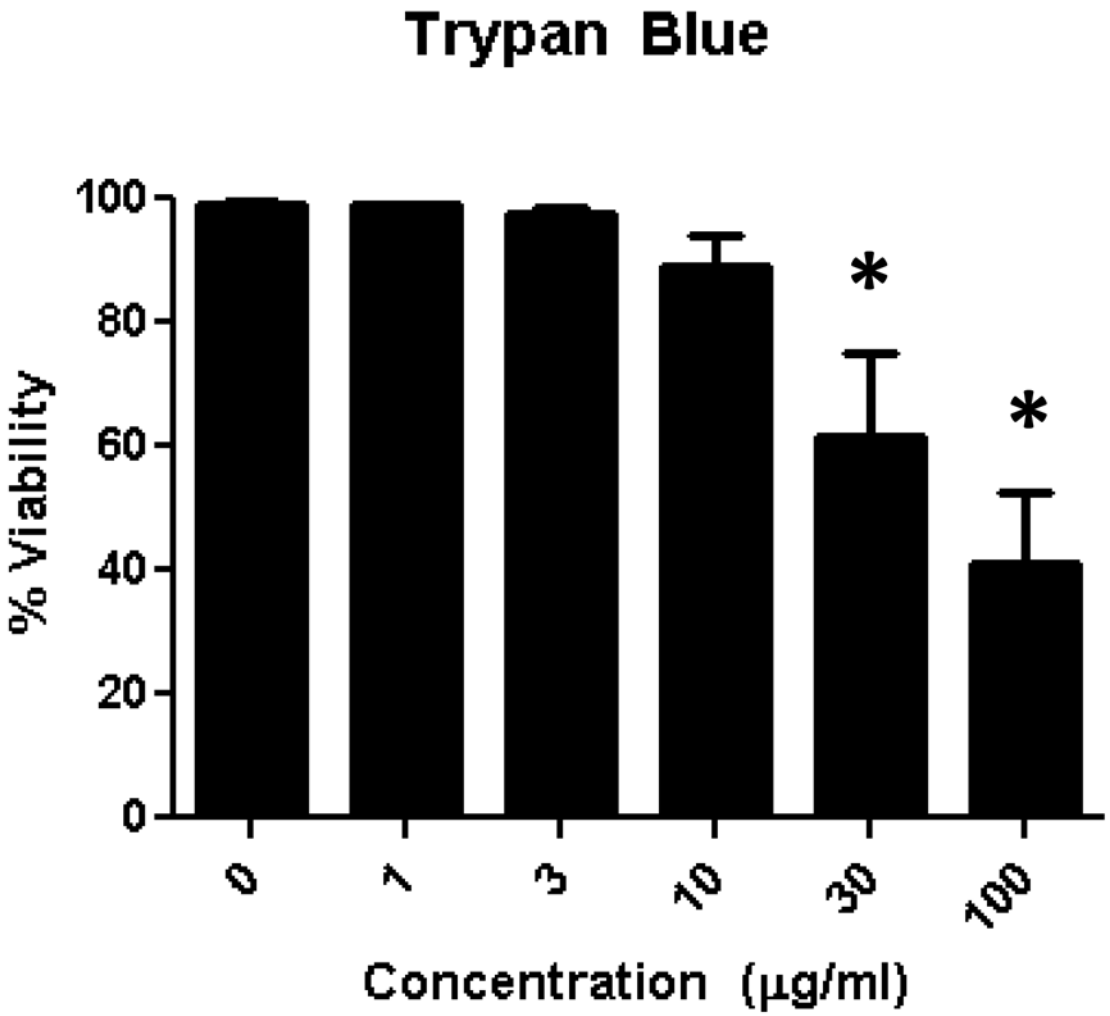

Figure 2.
Cell viability of human dermal fibroblasts treated with titanium dioxide nanoparticles using trypan blue dye exclusion assay. Data expressed as mean ± SD. *$p < 0.05$ compared to untreated control (0 μg/ml), n = 4.

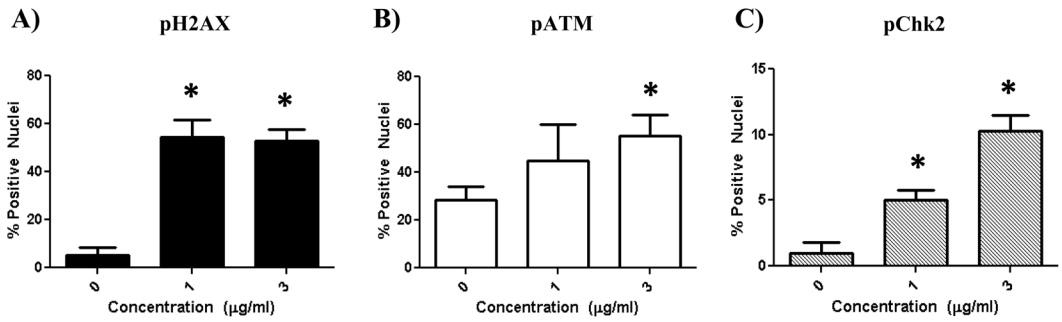

Figure 3.

Immunocytochemical analysis of titanium dioxide nanoparticle exposure in human dermal fibroblasts show phosphorylation of (A) H2AX (B) ATM, and (C) Chk2 after 24 h. Data expressed as mean ± SD. *$p < 0.05$ compared to untreated control (0 μg/ml), n = 3.

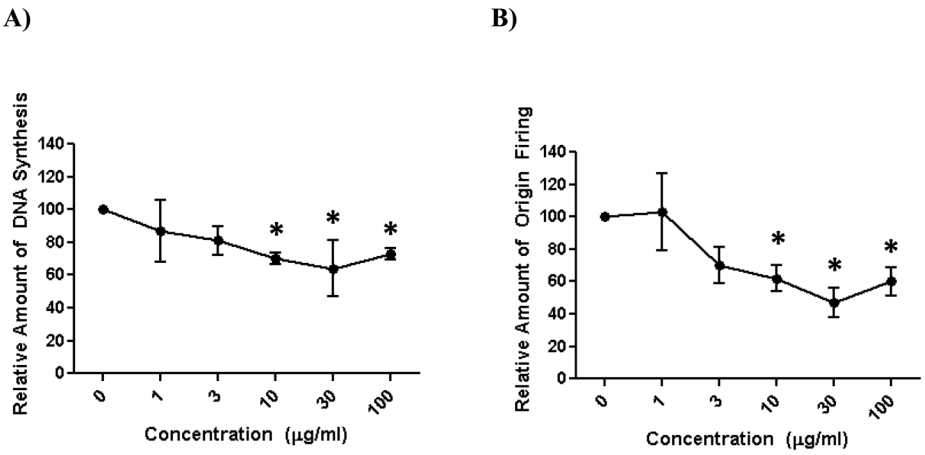

Figure 4.

Replication dynamics of DNA combed fibers after treatment of human dermal fibroblasts with titanium dioxide nanoparticles. Decreases were seen in A) relative DNA synthesis, as measured by relative length of green tracks in active replicons, and B) relative origin firing, as measured by number of green only tracks. Data expressed as % of untreated control. Data expressed as mean ± SD. *$p < 0.05$ compared to untreated control (0 μg/ml), n=3.

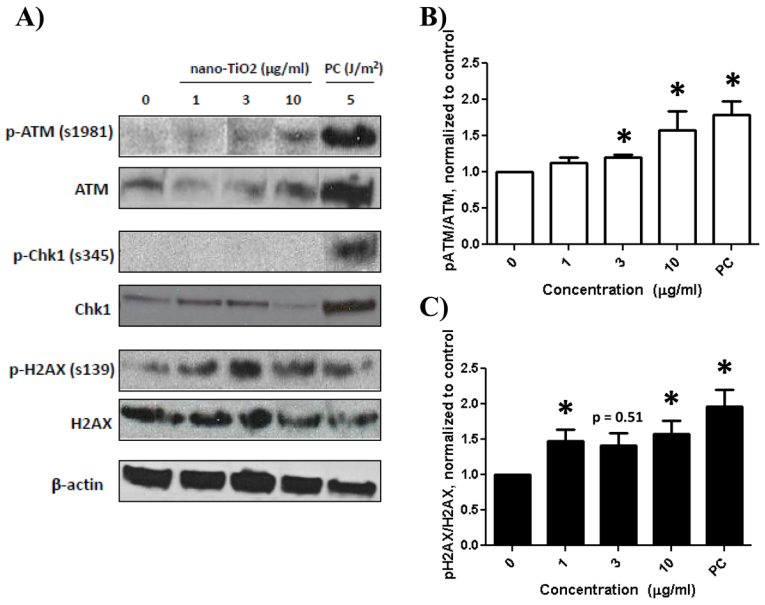

Figure 5.

A) Representative western blot of human dermal fibroblasts exposed to titanium dioxide nanoparticles for 24 h. Positive control (PC) used in all western blots was 5 J/m^2 UV-C. β-actin served as a loading control. Thephosphorylated/unphosphorylated ratio normalized to 0 μg/ml is shown for B) pATM/ATM and C) pH2AX/H2AX. Data expressed as mean ± SD. *$p < 0.05$ compared to untreated control (0 μg/ml), n=3.

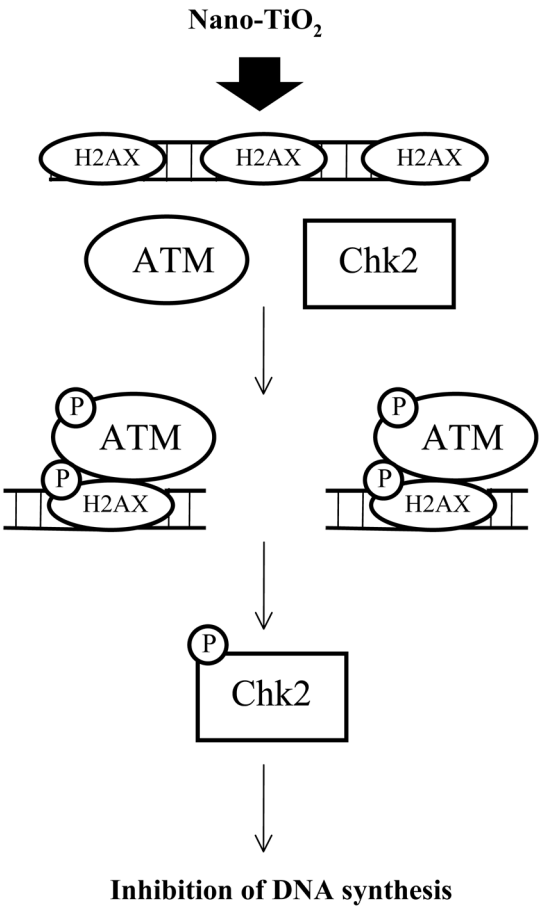

Figure 6.
Intra-S checkpoint signaling in response to titanium dioxide nanoparticle exposure for 24 hr.

Table 1

Size and zeta potential of nano-TiO_2 in cell culture medium (DMEM + 10% FBS) using dynamic light scattering. Data represented as mean ± SD of three independent experiments

Concentration (μg/ml)	Size (nm)	Zeta Potential (mV)
1	325.93 ± 10.34	−0.64 ± 0.51
3	314.37 ± 20.41	−0.48 ± 0.11
10	397.33 ± 17.48	−0.78 ± 0.05